Supporting information

Solvent/Temperature Dual-Responsive Photonic Crystal Structural Color Films Through Double Inverse Opal Structure

Shaorui He, Linmao Jia, Jiaxin Wang, Chaoran Xiao, Qian Yang and Zhaopeng Xu*
State Key Laboratory of Metastable Material Science and Technology, School of Information Science and Engineering, Yanshan University, Qinhuangdao, Hebei 066004, China
E-mail: xuzhaopeng1@163.com

S1. Experimental

Materials

Ammonia solution (28 wt%), Tetraethyl Orthosilicate (TEOS, 99 wt%), N, N′-methylene bis-(acrylamide) (BIS, 99 wt%), Acrylamide (98 wt%), N-isopropyl Acrylamide (NIPAM, 98 wt%) and Dimethyl Sulfoxide (DMSO, 99 wt%) were purchased from Shanghai Aladdin Biochemical Technology Co.Ltd. Ethanol (99.7 wt%), Acetone (99.5 wt%) and Hydrofluoric Acid (40 wt%) were purchased from Tianjin Kaitong Chemical Reagent Co. Ltd, and Hydrogen Peroxide (30% water solution) was purchased from Tianjin Kaitong Chemical Reagent Co. Ltd. All of the chemicals were purified before using. Glass slides (40×20 mm^2) were obtained from Weiss Experiment Products Co. Ltd, and washed with ethanol and acetone solution for 12 h, followed by being rinsed with ultrapure water in an ultrasonic bath for three times before usage.

Preparation of Monodisperse SiO_2 Spheres

SiO_2 colloidal spheres were prepared by a modified Stöber method. The size of SiO_2 colloidal spheres was controlled by tuning the amount of aqueous ammonia. After the reaction, the products were centrifuged and washed three times with ethanol (detailed information on the SiO_2 nanospheres is listed in Table S1). SiO_2 spheres with diameters of 250 and 320 nm were obtained. After sonicated for 1 h, the ethanol suspension of SiO_2 colloidal spheres (7 wt %) was obtained for subsequent dip-coating and spraying.

Fabrication of Patterned DIOPC Films Anticounterfeiting Structure

Different SiO_2 photonic crystal templates were prepared via the dip-coating method with 250 and 320 nm SiO_2 nanospheres. The different thicknesses of SiO_2 opal templates were formed by using dip-coating 2-5 times (see Fig. S1). The SiO_2 opal templates were placed within the working range of the Laser Marking machine (Diaotu DB1600). The working voltage of the Laser Marking machine is 12 V, and the wavelength of the emitted light is 445 nm. The letters

A and B were imported into the software. The light outlet of the Laser Marking machine was focused on the surface of the SiO_2 opal templates. The patterns were carved for about 1 minute. Finally, SiO_2 opal template A prepared by 320 nm SiO_2 nanospheres marked with letter A was obtained. SiO_2 opal template B prepared by 250 nm SiO_2 nanospheres marked with letter B was obtained. The combination of template A and template B formed a 'sandwich' structure where the gap between the two layers was separated by polyimide tape. Typically, the monomers NIPAM and cross-linking agent BIS were recrystallized to remove impurities. NIPAM (0.40 g) and AM (0.080 g) as monomers, Irg.124 (0.010 g) as the photo-initiator, BIS (0.0027 g) as the crosslinker were dissolved to obtain a pre-gel solution at 25°C. The pre-gel solution was aspirated and slowly injected into the gap between the 'sandwich' structure composed of the glass slide and the PC array. Under capillary force, the gaps between the nanospheres were filled with the precursor solution. Afterward, it was cross-linked under ultraviolet light (365 nm, 20 W) for 30 s to form a gel film. Then the 'sandwich' structure was incubated inside pure water until the gel film was automatically peeled off, and the photonic crystals gel film could be obtained. The resulting film obtained by Laser Marking and immersed in a 10 vol% hydrofluoric acid aqueous solution for 30 s and rinsed with deionized water several times.

Characterization of P(NIPAM-AM) Structural Color Films

SiO_2 microspheres were uniform spheres from the transmission electron microscopy (TEM) images in Fig. S1. The SiO_2 opal templates corresponding SEM images are shown in Fig. S2. It possesses a high-quality and typical face-centered cubic (fcc) close-packed structure. The reflection spectra of SiO_2 templates are shown in Fig. S3.

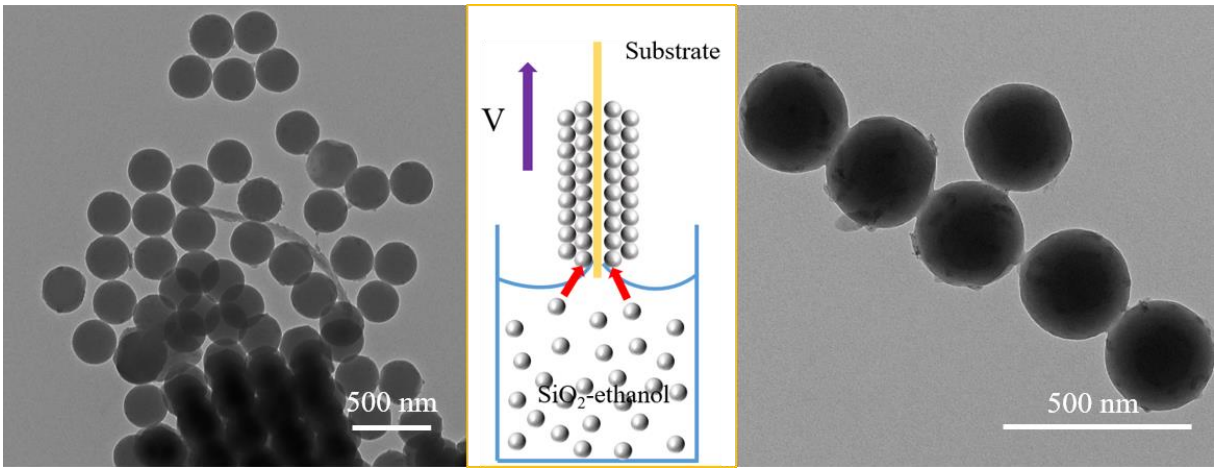

Fig. S1 The SiO_2 monodisperse nanospheres (the color of the reflected light of the corresponding assembled template is red and green, see Fig. S3) and the schematic illustration of the dip-coating method. 7 wt % SiO_2 ethanol dispersion was prepared for further use. The pulling rate of the dip-coating assembly process was 2 μm/s at 25°C.

According to Bragg-Snell's law, the PBGs of FCC-structured PCs can be theoretically calculated as:

$$\lambda_{max}=1.633D(n^2_{avg}-\sin^2\theta)^{1/2} \quad (1)$$

$$n^2_{avg}=0.74\times n^2_{SiO_2}+0.26\times n^2_{air} \quad (2)$$

where λ_{max} is the maximum reflected wavelength, θ is the incident angle, D is the diameter of the SiO_2 particles, n_{avg} is the effective refractive index, n_{SiO_2} = 1.45 and n_{air} = 1.0 are the refractive indexes of silica and air, respectively. We can calculate the micropore diameter roughly through Bragg-Snell's law of diffraction. The formula can be converted to:

$$D=\lambda_{max}/[1.63\times(1.82-\sin^2\theta)^{1/2}] \quad (3)$$

According to the maximum reflection wavelength in Fig. S3, the particle size of silica nanoparticles can be roughly estimated, and the estimated value is close to the actual value determined by SEM (see Table S1 and Fig. S2).

Table S1. The diameter of the SiO_2 particles and the maximum reflection wavelength of the film (theoretical and practical)

λ_{max} (nm)	θ (°)	Theoretical D (nm)	Practical D (nm)
520.5	90	267.8	~255.7
723.5	90	324.2	~318.3

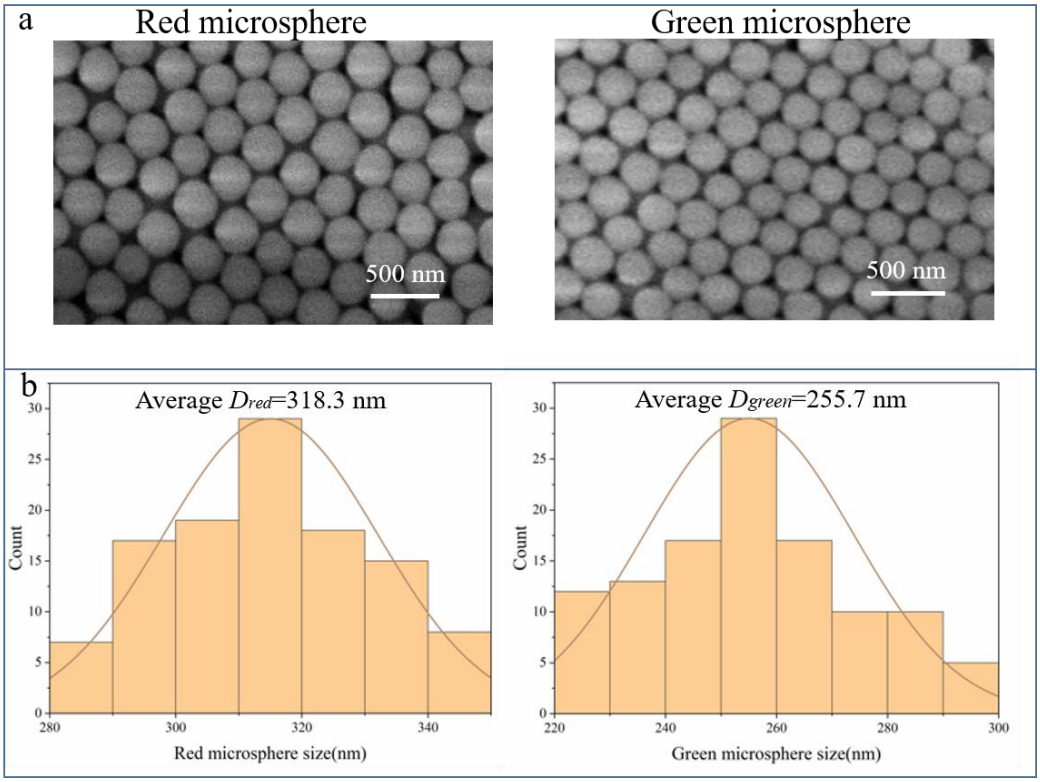

Fig. S2 a) SEM (top view) of opal photonic crystals assembled by silica microsphere with different particle sizes. b) The corresponding particle size statistics of silica microsphere, the average size is 318.3 and 255.7 nm, respectively. These are consistent with the theoretical calculation.

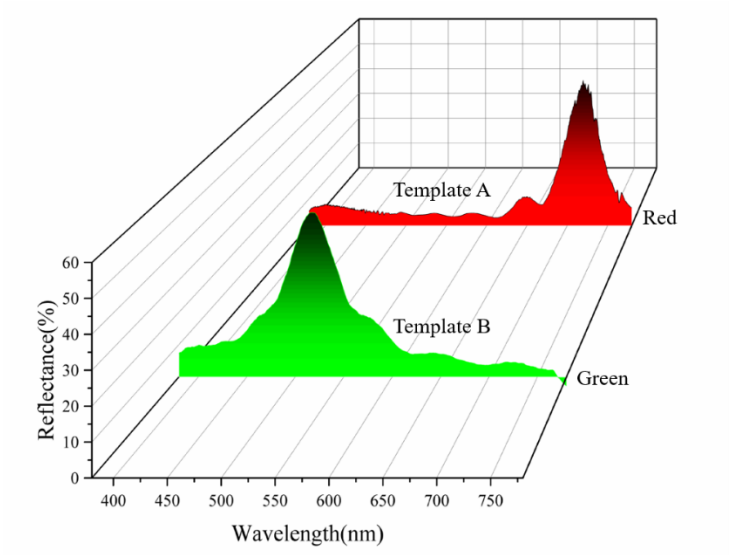

Fig. S3 Reflection spectra of the opal photonic crystals (template A and B). The maximum reflected wavelength is 723.5 and 520.5 nm, respectively.

S2. Comparative analysis of changing thickness of layer A and layer B. In double inverse opal photonic crystal (DIOPC), the reflected light of the top layer and the bottom layer inverse opal will produce superposition, forming a superimposed PBG. The superposed PBG is related to the thickness of the top layer and the bottom layer inverse opal.

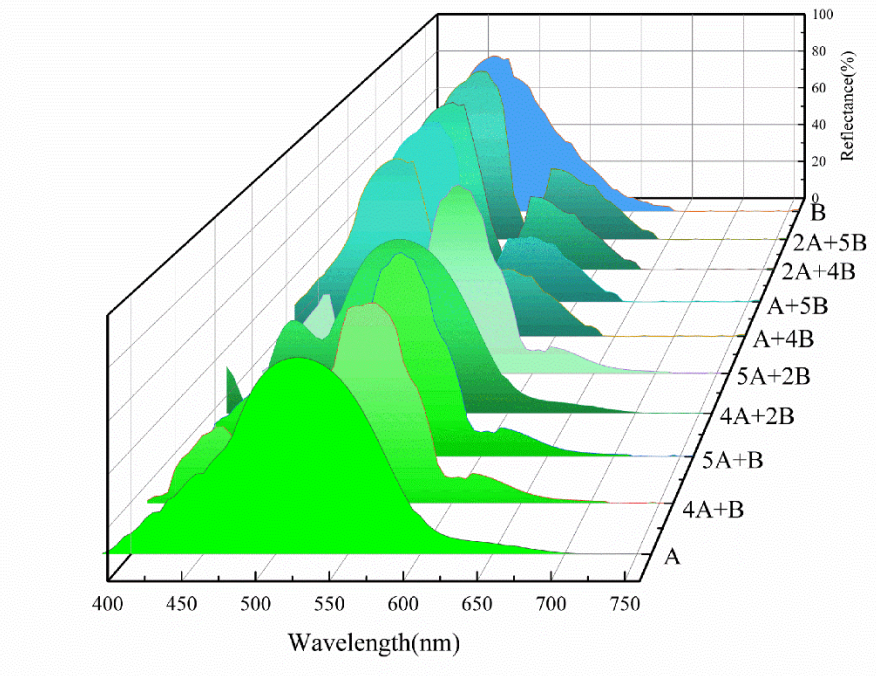

Fig. S4 Comparative analysis of changing thickness of layer A and layer B

As can be seen from Fig.S4, the maximum reflection peak corresponding to the layer A inverse opal template appears at 520 nm. The maximum reflection peak corresponding to the layer B inverse opal template appears at 463 nm. When layer A is upturned, the reflection spectrum of "4A+B" inverse opal photonic crystal (IOPC) structure color hydrogel film shows

a strong reflection peak at 542 nm, and only a weak secondary reflection peak at 433 nm, which can be approximately a single PBG. The reflection spectrum of "5A+B" IOPC structure color hydrogel film shows a strong reflection peak at 544 nm, and a very weak secondary reflection peak at 428 nm, which can be approximated as a single PBG. The reflection spectrum of "4A+2B" IOPC structure color hydrogel film shows a strong reflection peak at 527 nm, and only shows a strong secondary reflection peak at 431 nm, which can be approximated as double PBGs. The reflection spectrum of "5A+2B" IOPC structure color hydrogel film shows a strong reflection peak at 538 nm, and a very strong reflection peak at 427 nm, which can be approximated as double PBGs. When layer B is upturned, the reflection spectrum of "A+4B" IOPC structure color hydrogel film shows a strong reflection peak at 463 nm, and a weak secondary reflection peak at 543 nm, which can be approximately a single PBG. The reflection spectrum of "A+5B" IOPC structure color hydrogel film shows a strong reflection peak at 464 nm, and a very weak reflection peak at 558 nm, which can be approximated as a single PBG. The reflection spectrum of "2A+4B" IOPC structure color hydrogel film shows a strong reflection peak at 470 nm, and a strong secondary reflection peak at 541 nm, which can be approximated as double PBGs. The reflection spectrum of "2A+5B" IOPC structure color hydrogel film shows a strong reflection peak at 467 nm, and a strong secondary reflection peak at 537 nm, which can be approximated as double PBGs. According to the above results, the larger the thickness difference between the top and bottom IOPC structure color hydrogel films, the stronger the color superposition effect. However, if the thickness of the single-layer IOPC structure color hydrogel film is too thin, the secondary reflection peak is not obvious, causing the DIOPC film to resemble a single color more closely. Therefore, the "2A+4B" and "2A+5B" DIOPC films can flexibly realize the regulation of single and double PBGs.

S3. Ethanol Response for P(NIPAM-AM) Film. The "2A+4B" P(NIPAM-AM) film selectively displays the overlapping colors (blue-cyan) (A-B Mode, Fig. S5a, f, g).

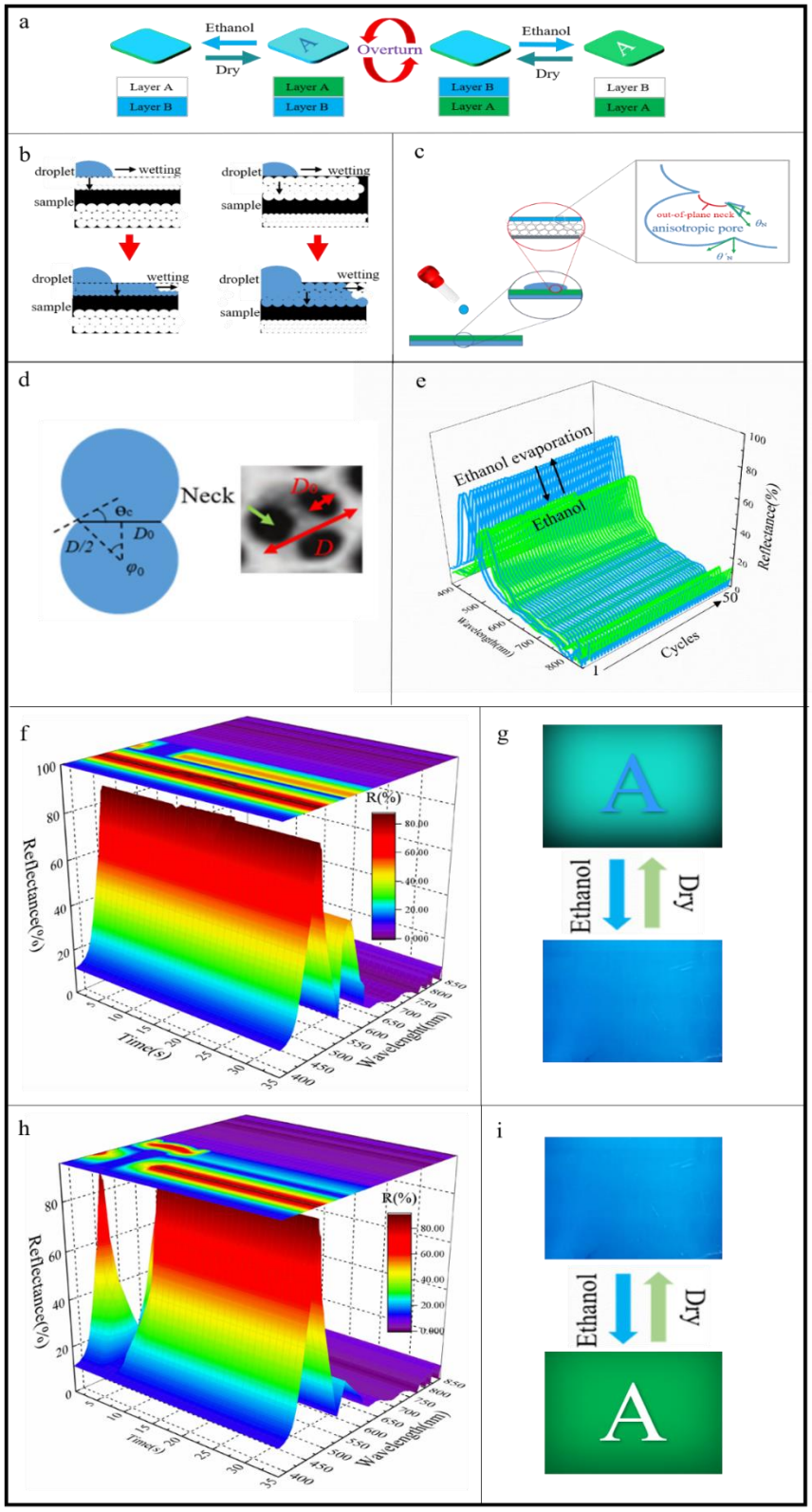

Fig. S5 a) Schematic of ethanol response for hiding and displaying letter A. b) Schematic diagram of anisotropic wetting phenomena, with arrows to indicate liquid motion. Anisotropic inverse opal film is wetted by 30 wt% ethanol. c) Schematic illustration of ethanol wetting front propagating at the neck of two micropores. d) The typical SEM image of the micropore and the neck and schematic illustrating the relationship between φ_0 and the wetting response. Infiltration occurs if the intrinsic contact angle (θc) is less

than φ_0, while no infiltration occurs if $\theta c > \varphi_0$. e) The reflection cycles of the 'B-A Mode' of the spectra (blue) in the ethanol response and evaporation. f) The reflectance spectra (blue-cyan) of the 'A-B Mode' during the process of the ethanol response. Since the response occurs almost instantaneously, the figure shows the change in the reflectance spectrum during the response and ethanol evaporation processes. The infiltration experiment started at t = 2 s by wiping with ethanol. g) and i) The corresponding optical photographs of the DIOPC film before and after the ethanol response (the background is a black table). h) The reflectance spectra of the 'B-A Mode' during the process of the ethanol response.

The film immediately appears blue and hides the letter A when wetted with 30 wt% ethanol. We hypothesized that all macropores are filled with ethanol whose refractive index ($n_{ethanol}$=1.36) is close to that of the P(NIPAM-AM) polymer ($n_{polymer}$≈1.44). When the 2A layer is wetted with ethanol, the film immediately appears blue and hides the letter A, there is an obvious reflection peak (469 nm) in the spectra. In addition, the film returns to its original blue-cyan and displays the letter A again with the evaporation of ethanol. When the 4B layer is upturned, the P(NIPAM-AM) film selectively displays the blue of the 4B layer (B-A Mode, Fig. S5a, h, i). The film immediately appears green and displays the letter A when wetted by ethanol. Moreover, the film returns to its original blue and hides the letter A with the evaporation of ethanol. Notably, the color shift in the hydrogel film is reversible, with the intensity and position of the reflection peaks remaining relatively stable after 50 cycles (see Fig. S5e). The effective refractive index increases during the infiltration of ethanol, according to Bragg-Snell's law, the PBG shows a redshift. The new peak appears in the near-infrared region (840 nm (for the A-B Mode) and 830 nm (for the B-A Mode)), so it cannot be seen by human eyes, the letter at the top of the film is hidden. According to the change in reflectance (Fig. S5f, h), when the top layer of the film is completely wetted by ethanol, the light scattering effect of the top layer to the bottom layer is greatly weakened. Since the refractive index of ethanol is larger than that of air, the scattering effect caused by PBG in the top layer shifts to the near-infrared region with the redshift of PBG. At the same time, due to the matching of refractive index, the top layer of the film is similar to a 'transparent glass', so that the reflected light of the bottom layer can penetrate the top layer smoothly, and the color of the film can be similar to the color of the bottom layer, suggesting that the 3D periodic structure was changed when the film was wetted by ethanol.

To explain the mechanism of ethanol-wetting response to DIOPC hydrogel film, the infiltration response mode in the ethanol-wetting process is further analyzed.[1] It can be measured by the neck Angle (φ_0) of the inverse opal.[2] The neck Angle is the central angle corresponding to the opening (neck) at the junction of two adjacent large holes in the inverse opal. The two opal pores are connected through the neck, and the liquid surface through the

neck shows concave curvature due to wetting resistance. To explain these properties, the inverse opal structure can be illustrated by abstracting it as a simple model with two spheres connected by small holes (see Fig. S5d). Fig. S5d shows the measured contact angle (θ) for ethanol on the flat film. Notably, the threshold between the nonwetted and wetted states occurs in the contact angle range in all cases, and the azimuthal angle of opening (φ_0) can be approximated as the contact angle.[3] The resistance to wetting down to such a low contact angle can be explained by the reentrant curvature associated with the narrow openings between adjacent pores. The schematic of the ethanol front advancing through a single unit of the film is shown in Fig. S5b,c. The azimuthal angle of opening (φ_0=arcsin(D_0/D)≈23.6°(for 'Layer A') to 24.6°(for 'Layer B')) was calculated according to its physical data (pore diameter D≈277.8 nm and the opening diameter D_0≈111.1 nm for 'Layer A', D≈257.6 nm and D_0≈103.4 nm for 'Layer B', see Fig. S5d). The change in free energy of the liquid-soaked opal is divided into two parts, one is the change in free energy caused by the replacement of the gas-solid interface by the liquid-solid interface (ΔG_1), and the other is the change in free energy caused by the increase/decrease of the liquid-gas interface (ΔG_2). It is generally assumed that the liquid-gas interface remains flat:

$$\Delta G_1 = \gamma_{\mathrm{la}}(\cos\theta_{\mathrm{c}})2\pi(\frac{D}{2})^2(\cos\varphi - \cos\varphi_0) \tag{4}$$

$$\cos\theta_{\mathrm{c}} = \frac{\gamma_{\mathrm{sa}} - \gamma_{\mathrm{sl}}}{\gamma_{\mathrm{la}}} \tag{5}$$

$$\Delta G_2 = \gamma_{\mathrm{la}}2\pi(\frac{D}{2})^2(\sin^2\varphi - \sin^2\varphi_0) \tag{6}$$

The total free energy can be expressed as ($\triangle G=\triangle G_1+\triangle G_2$):

$$\Delta G = \gamma_{\mathrm{la}}\pi(\frac{D}{2})^2[\sin^2\varphi - \sin^2\varphi_0 - 2(\cos\theta_{\mathrm{c}})(\cos\varphi_0 - \cos\varphi)] \tag{7}$$

where γ_{la} is the liquid-gas surface tension, D is the diameter of the inverse opal hole, φ is the central Angle of the solid-liquid-gas junction at any time, that is the central Angle corresponding to the liquid front, γ_{sa} is the solid-gas surface tension, γ_{sl} is the solid-liquid surface tension. After the liquid front passes through the neck of the adjacent inverse opal hole, in the process of continuous wetting, the area of the gas-liquid interface first increases and then decreases due to the curvature of the spherical hole. When the area of the gas-liquid interface increases ($\varphi>\varphi_0$), ΔG_2 is positive. In the process of wetting the liquid from the neck down, θ_{c}=23.1°<φ_0 (Figure S6). The liquid is well infiltrated in the inner wall of the inverse opal hole, and the free energy of wetting is always negative. At this point, the liquid spontaneously infiltrates the entire inverse opal.

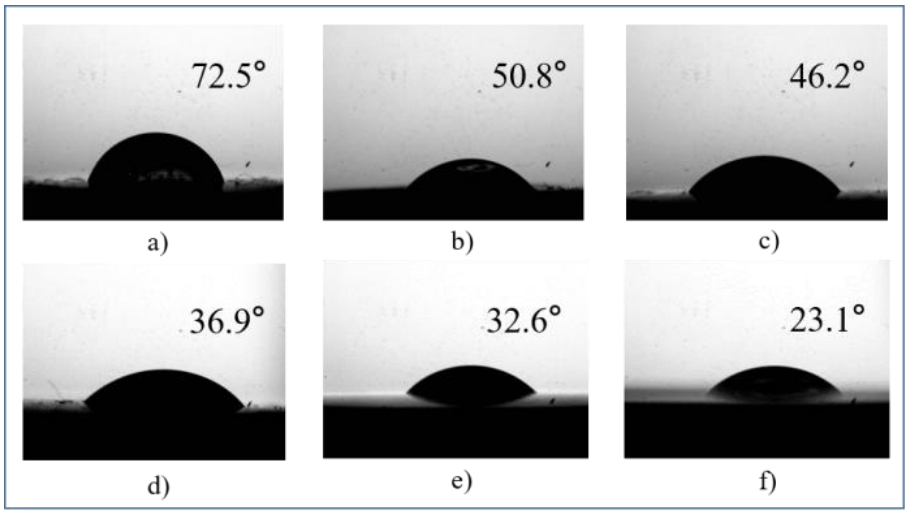

Fig. S6 The contact angle of deionized water and different ethanol concentrations on the surface of the DIOPC film. The weight percent from a) to f) are 0%, 10%, 15%, 20%, 25%, and 30%, respectively.

In addition, the "2B+4A" P(NIPAM-AM) hydrogel film is selected for ethanol response, and the P(NIPAM-AM) film selectively displays the overlapping colors (Fig. S7).

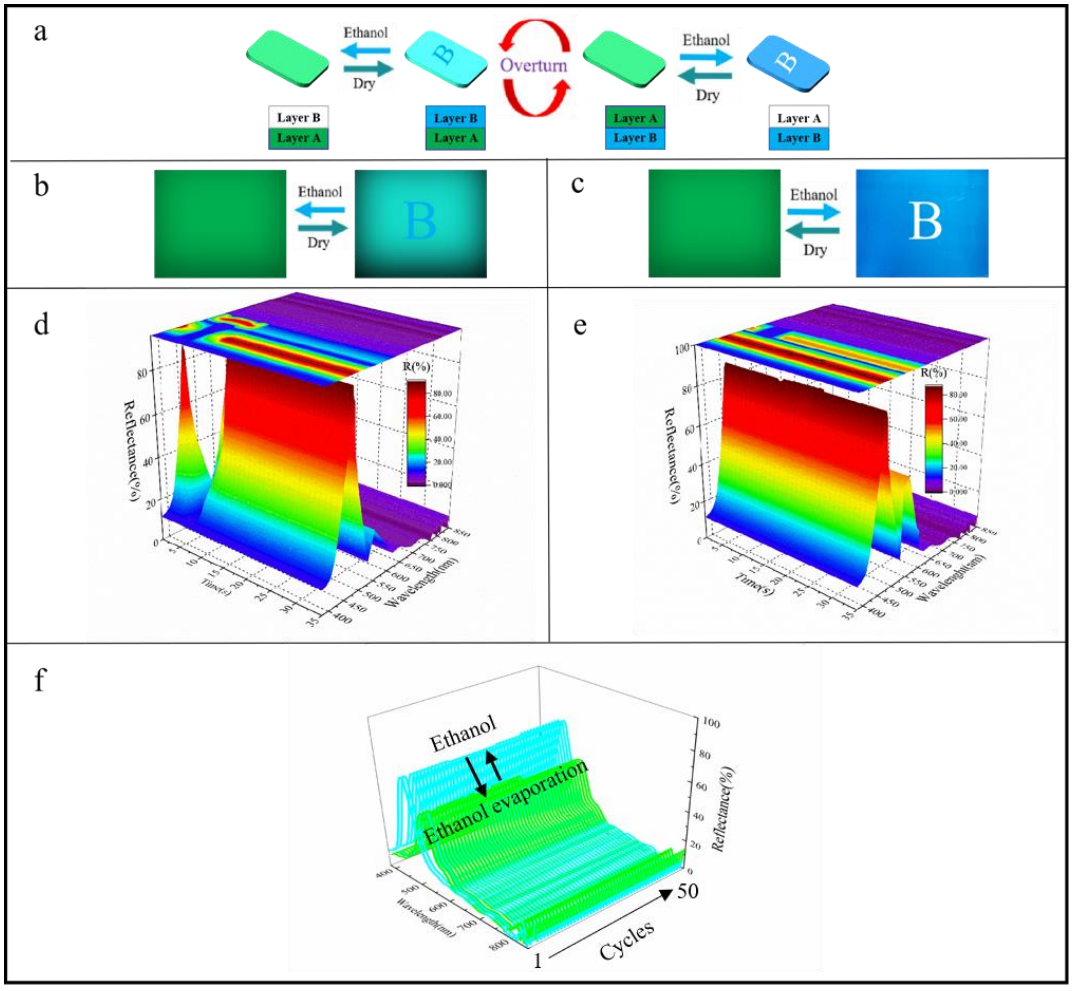

Fig. S7 a) Schematic of ethanol response for hiding and displaying letter B. b) and c) The corresponding optical photographs of the DIOPC film before and after the ethanol response (the background is a black table). d) The reflectance spectra of the 'B-A Mode' during the process of the ethanol response. Since the response

occurs almost instantaneously, the figure shows the change in the reflectance spectrum during the response and ethanol evaporation processes. The infiltration experiment started at t = 2 s by wiping with ethanol. e) The reflectance spectra of the 'A-B Mode' during the process of the ethanol response. f) The reflection cycles of the 'B-A Mode' of the spectra (blue) in the ethanol response and evaporation.

The film immediately appears cyan and hides the letter B when wetted by ethanol. We hypothesized that all macropores are filled with ethanol whose refractive index ($n_{ethanol}$=1.36) is close to that of the P(NIPAM-AM) polymer ($n_{polymer}$≈1.44). When the 2B layer is wetted by ethanol, there is an obvious reflection peak (455 nm) in the spectra. The hide and reproduction of the letter B is reversible through ethanol infiltration and evaporation. Most importantly, the intensity and position of the reflection peaks did not deviate significantly after 50 cycles (Fig. S6f). In addition, the film returns to its original cyan and displays the letter B again with the evaporation of ethanol. However, when the film is turned over, the P(NIPAM-AM) film selectively displays the green of the top layer (A-B Mode, Fig. S6a, c, e). The film immediately appears blue and displays the letter B when wetted by ethanol. Moreover, the film returns to its original green and hides the letter B with the evaporation of ethanol.

S4. Temperature Response for P(NIPAM-AM) Film. The P(NIPAM-AM) hydrogel will swell or shrink when its temperature approaches the Lower Critical Solution Temperature (LCST), exhibiting a clear and reversible bulk phase transition. Gel volume shrinkage is the result of the P(NIPAM-AM) chains dehydrating and aggregating into a densely packed spherical conformation as the ambient temperature rises above the LCST. This also strengthens the hydrophobic contacts between isopropyl groups. The hydrophilic amide groups' hydrogen bonds with water molecules balance out the hydrophobic interactions between the isopropyl groups when the surrounding temperature is below the LCST. The gel volume swells as a result of the polymer chains' flexible and stretched random coil shape.

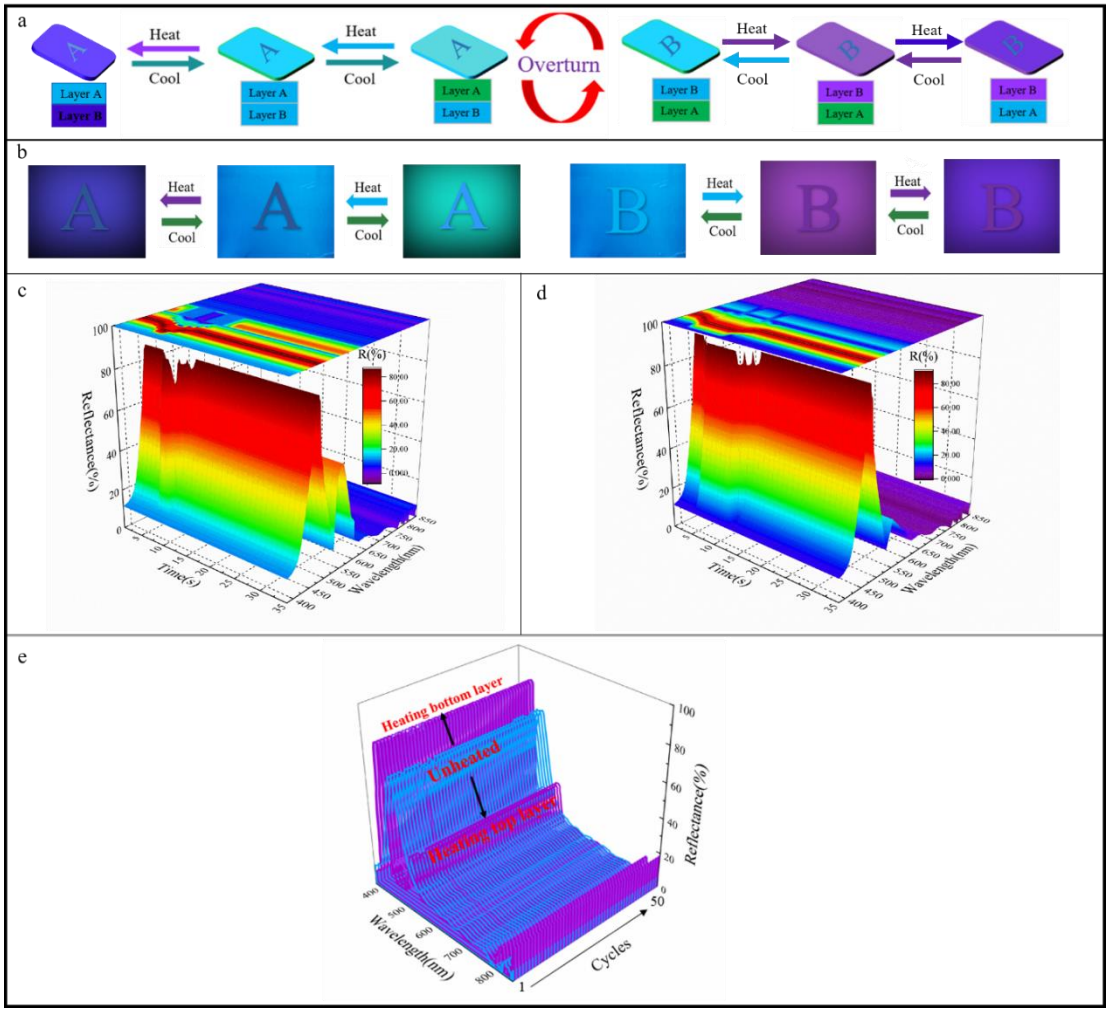

Fig. S8 a) Schematic of temperature response for displaying letters A and B. b) The corresponding optical photographs of the DIOPC film before and after the temperature response (the background is a black table). c) The reflectance spectra of the 'A-B Mode' during the process of the temperature response. The experiment started at t = 2 s by heating. d) The reflectance spectra of the 'B-A Mode' during the process of the temperature response. The experiment started at t = 2 s by heating. e) The reflection cycles of the 'B-A Mode' of the spectra (blue) in the temperature response.

The "2A+4B" P(NIPAM-AM) film selectively displays the overlapping color (A-B pattern, Fig. S8a, b, c). When the 2A layer of the hydrogel film is heated to 32℃, there is only a single peak in the reflection spectra in Fig. S8c. The film immediately appears blue and displays the letter A, and the reflection peak position appears at 470 nm. Then, when the whole hydrogel film is heated, the temperature of the bottom layer of the film increases, there are two photonic crystal reflection peaks in the reflection spectra, and the reflection peak position appears at 456 and 516 nm. The film immediately appears blue-purple and displays the letter A. In this process, the hydrogel film can shift from double PBGs (primary and secondary reflection peaks are 469 and 550 nm) to single PBG (reflection peak is 470 nm) and then double PBGs (primary and secondary reflection peaks are 428 and 492 nm), and the color of the hydrogel film changed

twice. When the 4B layer is upturned, the P(NIPAM-AM) film selectively displays only the blue of the 4B layer (B-A mode, Fig. S8a, b, d). Similarly, When the 4B layer of the hydrogel film is heated to 32℃, the reflection peak appears at 427 nm, and there is an obscure reflection peak at 550 nm. The whole hydrogel film appears light purple and displays the letter B. Then, when the whole hydrogel film is heated, there is still an obvious reflection peak in the reflection spectra, which appears at 429 nm, and an obscure reflection peak at 472 nm. The whole hydrogel film appears dark purple and displays the letter B. The intensity and position of the reflection peaks did not deviate significantly after 50 cycles (Fig. S8e).

In addition, the "2B+4A" P(NIPAM-AM) film selectively displays the overlapping colors (Fig. S9).

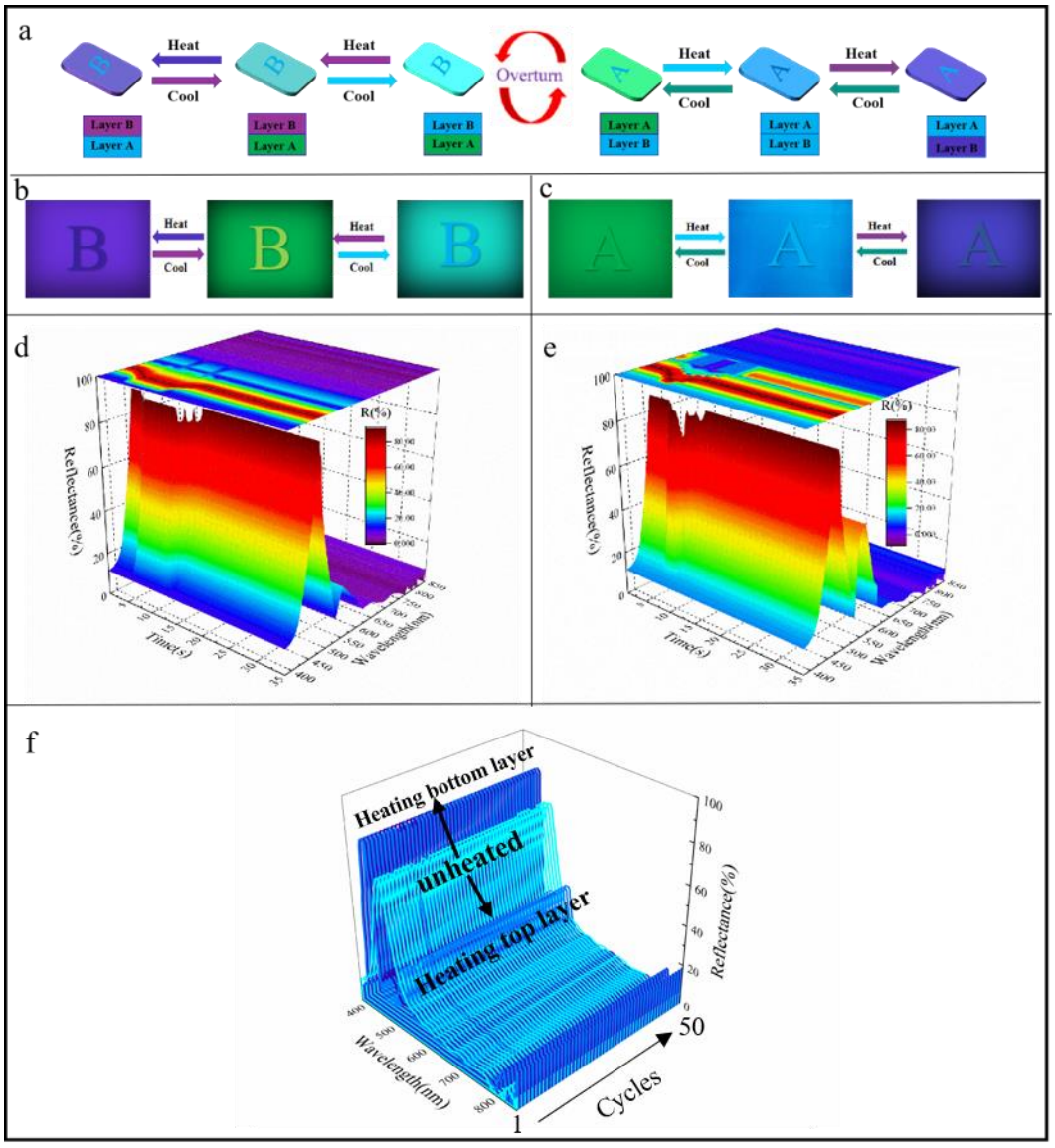

Fig. S9 a) Schematic of temperature response for displaying letters A and B. b) and c) The corresponding optical photographs of the DIOPC film before and after the temperature response (the background is a black table). d) The reflectance spectra of the ‘B-A Mode’ during the process of the temperature response. The

experiment started at t = 2 s by heating. e) The reflectance spectra of the 'A-B Mode' during the process of the temperature response. The experiment started at t = 2 s by heating. f) The reflection cycles of the 'A-B Mode' of the spectra (blue) in the temperature response.

When the 2B layer of the hydrogel film is heated to 32°C, there is only a single peak in the reflection spectra in Fig. S9d. The film immediately appears cyan and displays the letter B, and the reflection peak position appears at 534 nm. Then, when the whole hydrogel film is heated, the temperature of the bottom layer of the film increases, there are two photonic crystal reflection peaks in the reflection spectra, and the reflection peak position appears at 462 and 415 nm. The film immediately appears blue-purple and displays the letter B. In this process, the hydrogel film can shift from double PBGs (primary and secondary reflection peaks are 552 and 460 nm) to a single PBG (reflection peak is 534 nm) and then double PBGs (primary and secondary reflection peaks are 462 and 415 nm), and the color of the hydrogel film changed twice (Fig. S9a, b). When the 4A layer is upturned, the P(NIPAM-AM) film selectively displays the green of the 4A layer (Fig. S9a, c, e), and the reflection peak appears at 552 nm. Similarly, when the 4A layer of the hydrogel film is heated to 32°C, there is an obvious reflection peak at 462 nm. The whole hydrogel film appears blue and displays the letter A. Then, when the whole hydrogel film is heated, there is still an obvious reflection peak in the reflection spectra, which appears at 458 nm, and an obscure reflection peak at 412 nm. The whole hydrogel film appears dark purple and displays the letter A. The intensity and position of the reflection peaks did not deviate significantly after 50 cycles (Fig. S9f).

S10. Ethanol and Temperature Response for P(NIPAM-AM) Film. The "2B+4A" P(NIPAM-AM) film selectively displays the overlapping colors (cyan) (Fig. S10a).

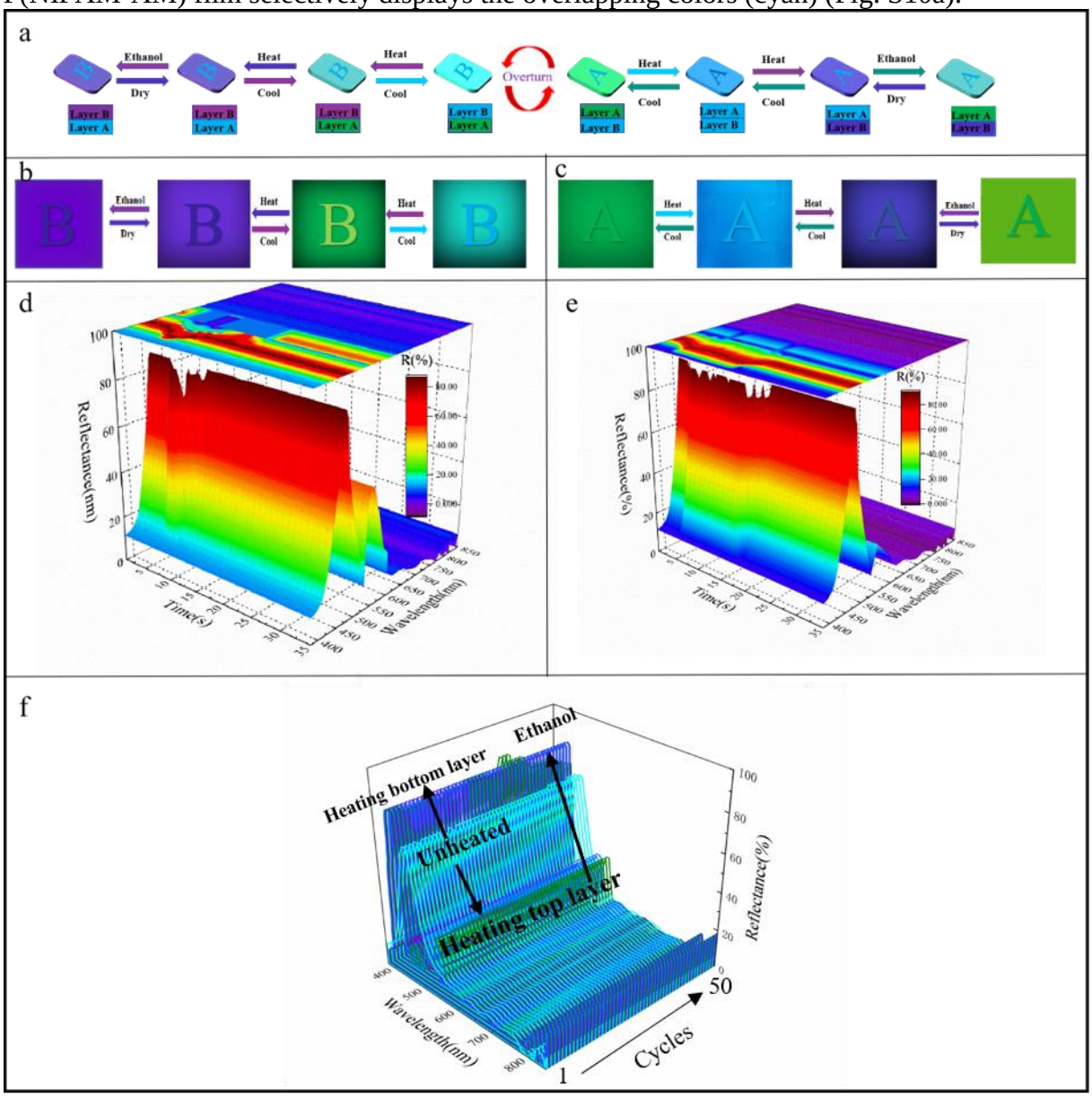

Fig. S10 a) Schematic of temperature and ethanol response for displaying letters B and A. b) and c) The corresponding optical photographs of the DIOPC film before and after the temperature and ethanol response (the background is a black table). d) The reflectance spectra of the 'B-A Mode' during the process of the temperature and ethanol response. The figure shows the change in the reflectance spectra during the heating and wetting processes. The infiltration experiment started at t = 3 s by heating and at t = 7 s by wetting. e) The reflectance spectra of the 'A-B Mode' during the process of the temperature and ethanol response. The infiltration experiment started at t = 3 s by heating and at t = 7 s by wetting. f) The reflection cycles of the 'A-B Mode' of the spectra in the temperature and ethanol response.

When the 2B layer of the hydrogel film begins to heat to 32°C, heat is transferred from the 2B layer to the 4A layer, and the color of the hydrogel film changes from cyan to blue-purple.

Subsequently, while maintaining the temperature at 32°C, the film is wetted by 30 wt% ethanol. The 2B layer of the film swells based on the previous contraction, but compared with the film without heating, the 2B layer of the film is still shrinking, the overall color of the film is light blue-purple and displays the letter B, with two reflection peaks (434 nm, 472 nm) evident in the reflection spectra. In this process (B-A mode, Fig. 10a, b, d), the hydrogel film transitions from double PBGs (552 nm, 460 nm) to single PBG (534 nm) to double PBGs (462 nm, 415 nm) and then to double PBGs (465 nm, 432 nm). When the 4A layer is upturned, the P(NIPAM-AM) film selectively displays the blue of the 4A layer (A-B mode, Fig. 10a, c, e). The 4A layer of the film expands following prior shrinkage, but compared with the film without heating, the 4A layer of the film is still shrinking, and the film immediately appears green-purple and displays the letter A. Throughout this process, the hydrogel film transitions from single PBG (552 nm) to single PBG (462 nm) to double PBGs (458 nm, 412 nm) and then to double PBGs (547 nm, 408 nm). The intensity and position of the reflection peaks did not deviate significantly after 50 cycles (Fig. S10f).

Supplementary theoretical analysis

Considering that the deformation scale of the hydrogel phase transition process is often in the super-large deformation range, the non-Gaussian property of the hydrogel chain segment is obvious, so the free energy form can be degraded as:

$$W = W_{\text{elastic}} + W_{\text{mix}} + W_{\text{ion}} \tag{8}$$

where W_{elastic} is the stretch free energy of the elastomeric network, W_{mix} is the mixture free energy of the network with solvent, and W_{ion} is the mixture free energy of ion with solvent.

$$W_{\text{elastic}} = -\frac{1}{2} N_c \mathrm{R}T \left\{ \begin{array}{l} \delta \ln \dfrac{\delta - \sum_{i=1}^{3} \lambda_i^2 - 3}{\delta} - \left(\dfrac{4}{f} - 2 \right) \ln J \\ - \dfrac{N_s}{N_c} \sum_{i=1}^{3} \left[\dfrac{(1+\eta)\lambda_i^2}{1+\eta\lambda_i^2} + \ln(1+\eta\lambda_i^2) \right] \end{array} \right\} \tag{9}$$

$$W_{\text{mix}} = \frac{\mathrm{R}T}{\upsilon_s} \left(\upsilon_s C_s \ln \frac{\upsilon_s C_s}{J} + \frac{\upsilon_s C_s}{J} \chi \right) \tag{10}$$

$$W_{\text{ion}} = \mathrm{R}T \sum_{\beta=l,+,-} C^{\beta} \left(\ln \frac{C^{\beta}}{\sum_{\beta=l,+,-} C^{\beta}} \right) \tag{11}$$

where N_c is the mole number of the cross-linked polymer chains, R is universal gas constant, T is absolute temperature, λ_i (i=1,2,3) are the stretches in principal direction, f is the junction functionality of the cross-links, J is the swelling ratio of the gel, N_S denotes the mole number of

the slip-links, η is the slippage parameter, υ_s is the molar volume of the solvent molecule, C_s is the mole number of the solvent molecules, C^β donates mole number of the species β, with subscripts "+" and "-" representing cations and anions, respectively.

First, assume that solid polymers, solutions, and ions cannot be compressed. Due to the low stress of hydrogels, the volume changed by molecular physical association is small relative to the volume changed by the absorption molecules. While the ion volume is much smaller than the solvent volume, the incompressibility condition can be expressed as $\upsilon_s C_s$. Since the solvent chemical potential in the equilibrium state must be constant, another form of free energy density function can be obtained by using the Legendre transformation:

$$\overline{W} = W - \mu C_s \tag{12}$$

To analyze the more general deformation behavior caused by the stimulation of the chemical-force coupling field, the above functions need to be expressed in the form of principal invariants I_i(i=1,2,3). Based on nonlinear continuum mechanics, when a hydrogel produces a large deformation in a coupled field, the principal invariant of the Cauchy-Green tensor ($C = F^T F$) can be expressed as:

$$I_1 = \mathrm{tr}C,\ I_2 = \mathrm{tr}C^2,\ I_3 = \det C = J^2 \tag{13}$$

Using the formula (1) - (6), the form of the energy density function can be obtained:

$$\overline{W} = -\frac{1}{2} N_c \mathrm{R}T \left\{ \delta \ln\left(\frac{I_1 - 3}{\delta} - 1 \right) - \frac{N_s}{N_c} \left[\ln\left(1 + \eta I_1 + \eta^2 I_2 + \eta^3 J^2 \right) \right] \right\} \tag{14}$$

For thermosensitive hydrogels, the dimensionless mixing parameters in the free energy function can be approximated as a function of the temperature and volume fraction of hydrogel φ.

$$\chi(T, \varphi) = \chi_0 + \frac{\chi_1}{1 + \upsilon_s C_s} = A_0 + B_0 T + \frac{(A_1 + B_1 T)}{J} \tag{15}$$

The parameter values of hydrogels are determined by the type of hydrogels, and the parameter values are different with different types. By fitting the experimental data, the specific values of each parameter can be obtained: A_0 = -10.857, B_0 = 0.04672K^{-1}, A_1 = 19.52, B_1 = -0.0572K^{-1}.

The results show that hydrogels in the swelling state can be simulated by the hyperelastic material model. Construct a hyperelastic frame and represent the nominal stress. For hydrogels, P_{ik} can be expressed as:

$$P_{iK} = \frac{\partial \overline{W}}{\partial F_{iK}} \tag{16}$$

Because the free swelling of the gel has isotropic properties, the stretch ratio in the three directions inside the gel is the same, then I_1=3$J^{2/3}$. Under the above conditions, according to

equation (7), the free swelling stretch ratio λ in a pure water solution should meet the following conditions:

$$N_c\upsilon_s(\lambda^{-1}-2\lambda^{-3}/4)+\ln(1-\lambda^{-3})+\lambda^{-3}+\frac{\chi_0}{\lambda^6}+\frac{\chi_1}{\lambda^9}=0 \tag{17}$$

A neutral P(NIPAM-AM) dry gel cube with a functional degree of 6 and a fixed charge density of 0 is an example to solve the phase transition temperature of the hydrogel. According to equation (15), the free energy density function of a cube in a swelling state can be expressed as:

$$\frac{\upsilon_s W}{\mathrm{R}T}=\frac{1}{2}N_c\upsilon_s\left[\delta\left(1-\frac{I_1-3}{\delta}\right)-\ln J\right]-\left[(J-1)\ln\left(\frac{J}{J-1}\right)-\frac{J-1}{J}\left(\chi_0+\frac{\chi_1}{J}\right)\right] \tag{18}$$

Because the free swelling of the gel has isotropic properties, the stretch ratio in the three directions inside the gel is the same, then $I_1=3J^{2/3}$. Under the above conditions, according to equation (14), the free swelling stretch ratio λ in a pure water solution should meet the following conditions:

$$N_c\upsilon_s(\lambda^{-1}-2\lambda^{-3}/4)+\ln(1-\lambda^{-3})+\lambda^{-3}+\frac{\chi_0}{\lambda^6}+\frac{\chi_1}{\lambda^9}=0 \tag{19}$$

The corresponding elastic entropy can be expressed as:

$$\Delta S_e=-\frac{1}{2}N_s\mathrm{R}\sum_{i=1}^{3}\left[\frac{(1+\eta)\lambda_i^2}{1+\eta\lambda_i^2}+\ln(1+\eta\lambda_i^2)\right] \tag{20}$$

It can be seen from equation (19) that with the increase of sliding parameters, the elastic entropy decreases and the corresponding elastic energy increases gradually. The effect of volume phase transition on the elastic energy tends to increase.

S11. The specific critical values

The specific critical values in Figure 3 (Manuscript) are shown in Tables S2, S3, and S4. (T-Temperature, υ_sC_1-The critical ethanol concentration of the hydrogel begins to swell rapidly, υ_sC_2-The critical solution concentration of the hydrogel changes from shrink to swell, υ_sC-ethanol concentration, T_1-The critical temperature of the hydrogel begins to shrink rapidly, T_2-The critical temperature of the hydrogel begins to shrink slowly, λ–The Swelling ratio of hydrogel when it changes from shrink to swell critical state)

Table S2. Relationship between P(NIPAM-AM) hydrogel swelling ratio and ethanol concentration at different temperature conditions

T(K)	$\upsilon_s C_1$	$\upsilon_s C_2$	λ
295	0.053	0.056	1
300	0.056	0.068	1
305	0.114	0.113	1

Table S3. Relationship between P(NIPAM-AM) hydrogel swelling ratio and ethanol concentration at different functional conditions

Degree of Functionality(φ)	$\upsilon_s C_1$	$\upsilon_s C_2$	λ
0	0.125	0.071	1
1	0.066	0.070	1
3	0.054	0.055	1

Table S4. Relationship between P(NIPAM-AM) hydrogel swelling ratio and temperature at different ethanol concentrations

$\upsilon_s C$	T_1(K)	T_2 (K)	λ
0.03	303	307	1
0.02	302	306	1
0.01	301	305	1
0.005	299	303	1

REFERENCES

1. I.-B. Burgess, L. Mishchenko, B.-D. Hatton, M. Kolle, M. Loncar, J. Aizenberg, *J. Am. Chem. Soc*., 2011, **133**, 12430-12432.

2. a) W. Hong, H.-R. Li, X.-B. Hu, B.-Y. Zhao, F. Zhang, D. Zhang, *Chem. Commun*., 2012, **48**, 4609-4611; b) W. Hong, H.-R. Li, X.-B. Hu, B.-Y. Zhao, F. Zhang, D. Zhang, Z. Xu, *Chem. Commun*., 2013, **49**, 728-730; c) I.-B. Burgess, N. Koay, K.-P. Raymond, M. Kolle, M. Loncar, J. Aizenberg, *ACS Nano*., 2012, **6**, 1427-1437; d) A. Marmur, *Langmuir*., 2003, **19**, 8343-8348.

3. a) J.-F. Bertone, P. Jiang, K.-S. Hwang, D.-M. Mittleman, V.-L. Colvin, *Phys. Rev. Lett*., 1999, **83**, 300; b) M. Qin, Y. Huang, Y.-N. Li, M. Su, B.-D. Chen, H. Sun, P.-Y. Yong, C.-Q. Ye, F.-Y. Li, Y.-L. Song, *Angew. Chem. Int. Ed*., 2016, **55**, 6911-6914.